cosmetics

MDPI

Article

Di (Isoquinolin-1-Yl) Sulfane (DIQS) Inhibits Melaninogenesis by Modulating PKA/CREB and MAPK Signaling Pathways

Jung Yoon Yang [1,†], Dae-Seop Shin [1,†], Kyu-Seok Hwang [1], Seong Soon Kim [1], Byung Hoi Lee [1], Se Hwan Ahn [2], Jin Hee Ahn [2] and Myung Ae Bae [1,*]

[1] Bio & Drug Discovery Division, Korea Research Institute of Chemical Technology, Daejeon 34144, Korea; yjy1608@krict.re.kr (J.Y.Y.); dsshin@krict.re.kr (D.-S.S.); kshwang@krict.re.kr (K.-S.H.); firstsay@krict.re.kr (S.S.K.); bnhlee@krict.re.kr (B.H.L.)

[2] Department of Chemistry, Gwangju Institute of Science and Technology, Gwangju 61005, Korea; ansehwan@gm.gist.ac.kr (S.H.A.); jhahn@gist.ac.kr (J.H.A.)

* Correspondence: mbae@krict.re.kr; Tel.: +82-42-860-7084

† These authors contributed equally to this work.

Abstract: The novel synthetic compound Di (isoquinolin-1-yl) sulfane (DIQS) was identified by zebrafish larva screening during the development of an agent to inhibit abnormal hyperpigmentation. In this study, we investigated the inhibitory effect of DIQS on melanogenesis and its underlying mechanism. DIQS inhibited melanin production and tyrosinase activity in B16F10 cells stimulated with α-melanocyte-stimulating hormone (α-MSH), as well as zebrafish embryos and reconstituted human skin tissue containing melanocytes. DIQS decreased the mRNA and protein expression of microphthalmia-associated transcription factor (*MITF*) and tyrosinase at a concentration of 10 μM. DIQS also inhibited the phosphorylation of cAMP response element-binding protein (CREB) and p-p38 and p-JNK stimulated by α-MSH. These results suggest that DIQS attenuates hyperpigmentation via inhibition of the cAMP/PKA/CREB/*MITF*/tyrosinase axis and MAPK pathways. Liquid chromatography–tandem mass spectrometry analysis revealed that DIQS blocked the conversion of tyrosine to L-3,4-dihydroxyphenylalanine (L-DOPA) in zebrafish embryos. Finally, we confirmed that DIQS was non-toxic in reconstituted human tissues such as the epidermis, used to test skin sensitization, and the cornea, used to test eye irritation. In summary, the results of this study suggest the potential of DIQS as a small-molecule agent for skin-whitening cosmetics and the treatment of hyperpigmentation disorders without biological toxicity.

Keywords: melanogenesis; *MITF*; tyrosinase; zebrafish; reconstituted human skin; skin-whitening

Citation: Yang, J.Y.; Shin, D.-S.; Hwang, K.-S.; Kim, S.S.; Lee, B.H.; Ahn, S.H.; Ahn, J.H.; Bae, M.A. Di (Isoquinolin-1-Yl) Sulfane (DIQS) Inhibits Melaninogenesis by Modulating PKA/CREB and MAPK Signaling Pathways. *Cosmetics* **2021**, *8*, 104. https://doi.org/10.3390/cosmetics8040104

Academic Editor: Lucia Panzella

Received: 29 September 2021
Accepted: 4 November 2021
Published: 5 November 2021

1. Introduction

Melanocytes are skin cells that produce black pigment, also known as melanin. Melanins form a complex group of heterogeneous biopolymers that are widely distributed in nature. Melanin is synthesized in melanosomes, which are organelles within melanocytes that can be transported to nearby keratinocytes to induce pigmentation [1,2]. Accumulated melanin in keratinocytes plays a crucial role in skin protection. For example, ultraviolet radiation from sunlight results in epidermal DNA photodamage, which can lead to mutations, immunosuppression, and consequent skin cancer [3]. Despite the skin-protective function of melanin, alterations in melanogenesis can also lead to various skin disorders. Hyper-pigmentation, such as senile lentigo, melanoderma, melasma, pigmented freckles, and pockmarks, involves the overproduction of melanin on the skin [4]. Hyperpigmentation is usually treated with melanin-specific laser equipment [5,6]. Nevertheless, these treatments are still associated with various side effects and have the disadvantage of being expensive. Therefore, the management of melanogenesis using cosmetic skin-whitening agents to inhibit pigmentary processes without unwanted side effects is an important target of cosmetic research [7].

Melanogenesis is regulated by several proteins including tyrosinase, tyrosine-related protein (TRP)-1, and *TRP-2* (also known as dopachrome tautomerase). Melanin biosynthesis is initiated by the oxidation of L-tyrosine to dihydroxyphenylalanine (DOPA) and subsequent catalysis of DOPA to DOPAquinone by tyrosinase. The resulting DOPAquinone serves as a substrate for the synthesis of eumelanin (black/brown) and pheomelanin (red/yellow) pigments. In eumelanin synthesis, DOPAchrome is catalyzed to dihydroxyindole-2-carboxylic acid by *TRP-2*, and *TRP-1* subsequently catalyzes the oxidation of dihydroxyin-dole-2-carboxylic acid to eumelanin [8]. Although three enzymes are involved in the melanogenesis pathway, tyrosinase activity is the most important protein in the melanin synthesis process. Transcription of tyrosinase, *TRP-1*, and *TRP-2* is regulated by microphthalmia-associated transcription factor (*MITF*), a transcription factor essential for melanocyte development, via a highly conserved motif [9–11]. CREB has been reported to regulate the expression of *MITF* in melanosomes, and the phosphorylation of CREB is regulated by the activation of cAMP/protein kinase A (PKA) cascades that play key roles in melanin synthesis [12]. Mitogen-activated protein kinase (MAPK) family proteins, including extracellular signal-regulated kinase (ERK) 1/2, c-Jun N terminal kinase (JNK) 1/2, and p38, also play important roles in melanogenesis [13].

In our previous study, zebrafish (*Danio rerio*) larvae were introduced as an animal replacement test model to identify the anti-melanogenic effects of various compounds and their mechanisms of action [14]. Di (isoquinolin-1-yl) sulfane (DIQS), one of the isoquinolin derivatives, was selected as a compound with an anti-melanogenic effect after the phenotype-based screening using zebrafish for 1000 compounds in Korea Chemical Bank. Various physiological effects of isoquinolin alkaloid derivatives are known in some studies. For example, scoulerine and cheilanthifoline, which are isoquinalkaloid derivatives, are known to exhibit the activities of anti-inflamatory, anti-bacterial effect, and anti-acetylcholinease [15]. Berberine, one of isoquinoline alkaloid derivatives, are known not only to have pharmacological properties such as anti-bacterial, anti-inflammatory, and anti-cancer, but also to inhibit melanin synthesis in α-MSH-stimulated B16F10 cells [16]. Moreover, the mechanism of action of berberine was associated with the inhibition of phosphorylation of PI3K/AKT, ERK, and GSK3β, suggesting that the physiological activity of isoquinolin derivatives was associated with MAPK pathway.

Zebrafish, which are small teleosts, have characteristic body striping patterns that contain three types of pigment cells: melanophores (black), xanthophores (yellow), and iridophores (containing reflecting platelets that result in the color blue). During embryonic development, melanocytes (called melanophores in fish) initially derive from the neural crest lineage, and molecular factors such as *Sox10*, *Mitf*, tyrosinase, and dopachrome tautomerase (Dct) are highly conserved in vertebrates including zebrafish [17]. And melanophores can be observed on the zebrafish surface during embryonic development allowing simple observation of the pigmentation process under microscopy. For this reason, anti-melanogenic compounds screening using zebrafish embryos is already well-established as an in vivo model [18]. A recent study using zebrafish models to demonstrate rhododendrol-induced leukoderma showed that zebrafish can be widely applied in skin pigmentation studies [19]. In this study, we demonstrated the anti-melanogenic effects of DIQS in a variety of experimental systems such as zebrafish- and human-derived artificial skin tissues, as well as mammalian melanoma cells. In addition, a fundamental mechanism for regulating anti-melanogenic activity was presented. The findings suggest that DIQS, which inhibits melanin production in a dose-dependent manner, could be used as a whitening agent in cosmetics.

2. Materials and Methods

2.1. Reagents

Arbutin, α-MSH, 1-phenyl 2-thiourea (PTU), L-DOPA and all other reagents were purchased from Sigma-Aldrich (St. Louis, MO, USA). Antibodies specific to *MITF*, tyrosinase,

TRP-1, *TRP-2*, and glyceraldehyde 3 phosphate dehydrogenase (*GAPDH*) were obtained from Santa Cruz Biotechnology (Santa Cruz, CA, USA).

2.2. Cell Culture

B16F10 murine melanoma cells were purchased from the American Type Culture Collection. Cells were grown as monolayers in Dulbecco's modified Eagle's medium (Gibco-BRL, Grand Island, NY, USA) supplemented with 10% fetal bovine serum (Gibco-BRL, Grand Island, NY, USA) and 1% penicillin/streptomycin (Gibco-BRL, Grand Island, NY, USA) at 37 °C in a humidified atmosphere with 5% CO_2 (NuAire, Plymouth, MN, USA).

2.3. Culture of Reconstituted Human Tissues

The Neoderm-ME, Neoderm-ED, and Neoderm-CD reconstituted human skin and cornea models (Tego Science, Seoul, Korea) were maintained according to the manufacturer's instructions. Briefly, the tissues were removed from medium-containing agar and transferred to 12-well plates, followed by incubation at 37 °C in a 5% CO_2 incubator (NuAire, Plymouth, MN, USA) for 24 h. Neoderm-ME was used to measure tyrosinase activity and melanin content. Neoderm-ED and Neoderm-CD were used to determine skin and eye irritation, respectively.

2.4. Maintenance of Zebrafish

Wild-type zebrafish were obtained from the Zebrafish Center for Disease Modeling (ZCDM) of Chungnam University (Daejeon, Korea). Zebrafish were maintained under standard conditions as described previously [20]. All experimental protocols involving zebrafish were approved by the Animal Care and Use Committee of the Korea Research Institute of Chemical Technology (KRICT-7B-ZF1).

2.5. Measurement of Melanin Content and Tyrosinase Activity in B16F10 Murine Melanoma Cells

To measure melanin content, B16F10 cells were washed with Dulbecco's phosphate-buffered saline (DPBS), detached using trypsin-EDTA, and counted using a hematocytometer. Cells (5×10^5) were dissolved in 1 N NaOH at 80 °C for 2 h. The cell lysates were centrifuged at 10,000× *g* for 10 min (Centrifuge 5415R, Eppendorf, Hamburg, Germany) and the supernatants were transferred to a 96-well plate for optical density measurements at 405 nm using a microplate reader (M1000PRO, TECAN, Mannedorf, Switzerland). For the tyrosinase activity assay, B16F10 cells were lysed in 0.1% Triton X-100 (in DPBS) and CelLytic™ M solution (Sigma-Aldrich, St. Louis, MO, USA), respectively. Lysates were clarified by centrifugation for 5 min at 10,000× *g*. After protein determination, lysates containing 2500 μg/100 μL protein were transferred to a 96-well plate, and 50 μL 10 mM L-DOPA in DPBS was added. The mixtures were incubated for 3 h at 37 °C, and the absorbance at 475 nm was measured.

2.6. Measurement of Melanin Content and Tyrosinase Activity in Neoderm-ME

Melanin content and tyrosinase activity were measured according to the slightly modified methods in previous studies [14,21]. Neoderm-ME was washed with DPBS and dissolved in 1 N NaOH at 95 °C for 45 min. The debris was clarified by centrifugation at 10,000× *g* for 10 min. The optical density of the supernatants was measured at 405 nm using a microplate reader. For the tyrosinase activity assay, Neoderm-ME tissue was lysed in 0.1% Triton X-100 (in DPBS) and CelLytic™ M solution, respectively. Lysates were clarified by centrifugation for 5 min at 10,000× *g*. After protein determination, lysates containing 2500 μg/100 μL protein were transferred to a 96-well plate, and 50 μL 10 mM L-DOPA in PBS was added. The mixtures were incubated for 3 h at 37 °C, and the absorbance at 475 nm was measured.

2.7. Measurement of Melanin Content and Tyrosinase Activity in Zebrafish Embryos

Phenotype-based evaluation using zebrafish embryos was conducted as described previously, with modifications [14,22]. To measure melanin content, approximately 200 zebrafish embryos were dissolved in 1 mL 1 N NaOH at 100 °C for 30 min and then vigorously vortexed to solubilize the melanin. The sample was transferred to a 96-well plate, and absorbance was measured at 490 nm. The results were calibrated using a standard curve constructed from known concentrations of synthetic melanin. For the tyrosinase assay, zebrafish embryos were lysed in CelLytic^{TM} M solution. The lysate was separated by centrifugation at 12,000× *g* for 5 min. The concentration of the protein was measured using the Bradford assay. The supernatants (2500 µg/100 µL protein) were transferred to a 96-well plate, and 100 µL 1 mM L-DOPA was added to each well. The microplate was incubated at 37 °C for 1 h, and absorbance was measured at 475 nm.

2.8. Measurement of Tyrosine and L-DOPA in Zebrafish Embryo

Triplicates of 20 embryos at 10 h post-fertilization were exposed to 0.2 mM PTU or various concentrations of DIQS (1, 5, 10, or 20 µM) in medium and incubated at 28 °C for 24 and 48 h. The embryos were manually detached from the chorion and anesthetized on ice for 10 min, washed three times with ice-cold PBS, and carefully removed from the supernatant. Wet embryos were lysed by snap-freezing three times in liquid nitrogen, followed by the addition of 300 µL distilled water and then ultrasonic probe sonication for 5 s on ice. Each embryo homogenate contained the same amount of total protein (µg/mg, whole embryo) for each sample, and protein was precipitated by adding an equal amount of methanol. Internal tyrosine and L-DOPA were extracted by vortexing for 5 min and centrifuging for 10 min at 13,000× *g* and 4 °C; the final supernatants were stored at −20 °C until analysis.

2.9. Liquid Chromatography Mass Spectrometry (LC-MS/MS) Analysis

Quantitative analysis of tyrosine and L-DOPA was performed by high-performance liquid chromatography combined with hybrid triple quadrupole mass spectrometry (LIT QTRAP 4000; AB Sciex, Foster City, CA, USA). The mobile phase consisted of 0.1% formic acid in water (eluent A) and 0.1% formic acid in acetonitrile (eluent B), followed by linear gradient elution (*v*/*v*) as follows: 2% A from 0 to 0.01 min, increasing to 60% A; at 5 min, equilibration to initial condition within 3.5 min at a flow rate of 300 µL/min and a run time of 9 min. Chromatographic separation was conducted using an Amide column (50 × 2.1 mm i.d., 3.5 µm; Waters, Milford, MA, USA) with an Amide guard column (3.9 × 5 mm i.d., 3.5 µm; Waters) at 35 °C. The multiple reaction monitoring mode and electrospray positive ionization were used for quantification of tyrosine and L-DOPA as follows: 182.1 → 136.1, 198.1 → 152.1 of ionic transition [23]. The optimized mass parameters included an ion spray voltage of 5500 V, source temperature of 550 °C, curtain gas of 50 psi, nebulizing gas (GS1) of 50 psi, and heating gas (GS2) of 50 psi.

2.10. In Vitro Skin Irritation Test

We maintained the Neoderm-ED reconstituted human skin model (Tego Science, Seoul, Korea) according to the manufacturer's instructions. Neoderm-ED was used to determine the skin irritation potential of test compounds in experiments performed according to Organization for Economic Cooperation and Development (OECD) Guideline 439 [24]. Briefly, Neoderm-ED was exposed to 90 µL fresh medium containing the test compound and incubated for 60 min at 37 °C in a 5% CO_2 incubator. After treatment, the tissues were stringently rinsed with PBS to completely remove the test compound. The inserts were transferred to cell culture plates containing fresh medium and incubated for 42 h at 37 °C in a 5% CO_2 incubator. At the end of the incubation period, tissue viability was determined by 3-[4,5-dimethylthiazol-2-yl]-2,5-diphenyl-tetrazolium bromide (MTT) assay. Inserts containing tissues were transferred to cell culture plates containing 2 mL MTT solution (0.3 mg/mL) and incubated for 3 h at 37 °C in a 5% CO_2 incubator. To terminate

the reaction, tissues were detached using an 8-mm biopsy punch (Kai Industries, Gifu, Japan) and submerged in 500 µL 0.04 N isopropanol. After 4 h of extraction, the optical density of the isopropanol extracts was determined photometrically at 570 nm.

2.11. In Vitro Eye Irritation Test

We maintained the Neoderm-CD reconstituted human cornea model (Tego Science, Seoul, Korea) according to the manufacturer's instructions. Neoderm-CD was used to determine the eye irritation potential of test compounds in experiments performed according to OECD Guideline 492 [25]. Briefly, Neoderm-CD was exposed to 30 µL test compounds diluted with fresh Ca^{2+}/Mg^{2+}-free PBS and incubated for 30 min at 37 °C in a 5% CO_2 incubator. Following treatment, tissues were rinsed twice with PBS to completely remove the test compound. The inserts were transferred to cell culture plates containing fresh medium and incubated for 30 min at 37 °C in a 5% CO_2 incubator. At the end of the incubation period, tissue viability was determined by MTT assay. Inserts containing tissues were transferred to cell culture plates containing 2 mL MTT solution (1 mg/mL) (Sigma-Aldrich, St. Louis, MO, USA) and incubated for 3 h at 37 °C in a 5% CO_2 incubator. To terminate the reaction, tissues were detached from the insert well and submerged in 1.5 mL isopropanol. After 4 h of extraction, the optical density of the isopropanol extracts was determined photometrically at 570 nm.

2.12. Reverse Transcription-Quantitative Polymerase Chain Reaction (RT-PCR)

B16F10 melanoma cells (5×10^5) were seeded in a 60-mm cell culture plate and incubated at 37 °C for 24 h. Cells were treated with 500 µM Arbutin and various concentrations of DIQS (1, 5, and 10 µM) for 48 h. Total RNA was isolated from B16F10 cells using the TRIzol reagent (Invitrogen, Carlsbad, CA, USA). The concentration of the isolated RNA was measured using the NanoQuant plate and microplate reader (M1000PRO, TECAN, Mannedorf, Switzerland). The reactions were conducted in the MicroAmp Fast Optical 96-Well Reaction Plate sealed with MicroAmp optical adhesive film (Life Technologies, Carlsbad, CA, USA). The primer pairs used are shown in Table 1. Reverse-transcription quantitative polymerase chain reaction (qRT-PCR) analysis was performed using Verso SYBR Green 1-Step qRT-PCR Low ROX Mix (Thermo Scientific, Cambridge, MA, USA) on the 7500 Fast Real-Time PCR System (Applied Biosystems, Life Technologies, Carlsbad, CA, USA). Expression levels were analyzed using the ΔΔCT method normalized to *GAPDH* (mouse).

Table 1. Primer sequences for RT-PCR analysis.

Gene		Sequence
MITF	Forward	5′-AACAAGGGAACCATTCTCAAGG-3′
	Reverse	5′-AGATCAGGCGAGCAGAGACC-3′
Tyrosinase	Forward	5′-CTCTGGGCTTAGCAGTAGGC-3′
	Reverse	5′-GCAAGCTGTGGTAGTCGTCT-3′
TRP-1	Forward	5′-GCTGCAGGAGCCTTCTTTCTC-3′
	Reverse	5′-AAGACGCTGCACTGCTGGTCT-3′
TRP-2	Forward	5′-GTCCTCCACTCTTTTACAGACG-3′
	Reverse	5′-ATTCGGTTGTGACCAATGGGT-3′
GAPDH	Forward	5′-GAGAACTTTGGCATTGTGG-3′
	Reverse	5′-ATGCAGGGATGATGTTCTG-3′

2.13. Western Blot Analysis

B16F10 melanoma cells (5×10^5) were seeded in a 60-mm cell culture plate and incubated at 37 °C for 24 h. Cells were treated with 500 µM Arbutin and various concentrations of DIQS (1, 5, and 10 µM) for 48 h. Radioimmunoprecipitation lysis buffer (Thermo Scientific, Rockford, IL, USA) containing protease inhibitor cocktail (Thermo Scientific, Waltham, MA, USA) was used to prepare whole-cell lysates, which were then centrifuged

at 16,100× g for 30 min at 4 °C. The supernatants were collected, and the protein concentration was determined using the Bradford assay. Proteins (60 μg) were resolved using 4–12% Bis-Tris and SDS–PAGE (Thermo Scientific, Rockford, IL, USA) and transferred to a polyvinylidene fluoride membrane. The membranes were blocked with 5% skim milk in Tris-buffered saline containing 0.1% Tween 20 (TBS-T) solution and then incubated with the specific primary antibodies in TBS-T for 3 h at room temperature. Blots were washed with TBS-T and then incubated for 30 min with a secondary antibody. Protein bands were visualized using the SuperSignal West Femto Maximum Sensitivity substrate (Thermo Scientific, Waltham, MA, USA) on the MyECL imager (Thermo Scientific, Waltham, MA, USA).

2.14. Statistical Analysis

Data are presented as means ± standard deviation (SD). An unpaired t-test was used to analyze differences compared with the dimethyl sulfoxide (DMSO) group, and statistical significance was determined at * $p < 0.05$ and ** $p < 0.01$. All statistical analyses were performed using GraphPad Prism v.8.4.3 (GraphPad Software, 2020, San Diego, CA, USA).

3. Results

3.1. DIQS Induced Anti-Melanogenic Activity in B16F10 Melanoma Cells

DIQS is one of the derivatives containing two isoquinoline, as shown in Figure 1A. DIQS was identified as a compound with an anti-melanogenic effect in phenotype-based screening using zebrafish. Based on the results of various pharmacological activities and anti-melanogenic effects by previously reported isoquinolin derivatives, this study attempted to investigate the mechanism of action representing the anti-melanogenic effect of DIQS and its efficacy/safety for use in the cosmetics industry. First, we explored any potential cytotoxic effects of DIQS in the context of its potential use as a cosmetic agent. We performed cell viability assays to determine the in vitro cytotoxicity of DIQS in B16F10 melanoma cells. Cells were treated with 0.1–20 μM DIQS for 48 h. No significant cytotoxicity was observed in cells treated with DIQS at concentrations of 0.1–10 μM (Figure 1B). To determine the effect of DIQS on α-MSH-induced melanin synthesis, we evaluated the melanin content of the B16F10 cells photometrically. The melanin content of α-MSH-stimulated B16F10 cells was markedly reduced after DIQS treatment (Figure 1C,D). Tyrosinase is a key enzyme involved in melanin synthesis. The inhibition of tyrosinase activity in cells is a prerequisite for candidates exhibiting anti-melanogenic effects. DIQS significantly inhibited tyrosinase activity in α-MSH-stimulated B16F10 cells at a concentration of 10 μM (Figure 1E), at which tyrosinase activity induced by α-MSH was decreased by approximately 37.2%. This inhibitory effect was similar to that of 500 μM arbutin used as a positive control.

3.2. DIQS Affected the mRNA and Protein Levels of Melanogenesis-Related Factors

Next, we measured the mRNA and protein levels of *MITF*, tyrosinase, *TRP-1*, and *TRP-2* to evaluate the inhibitory mechanism of DIQS in melanogenesis. B16F10 cells were stimulated with α-MSH for 48 h with or without DIQS at various concentrations. The mRNA levels of *MITF*, tyrosinase, *TRP-1*, and *TRP-2* were examined by qRT-PCR.

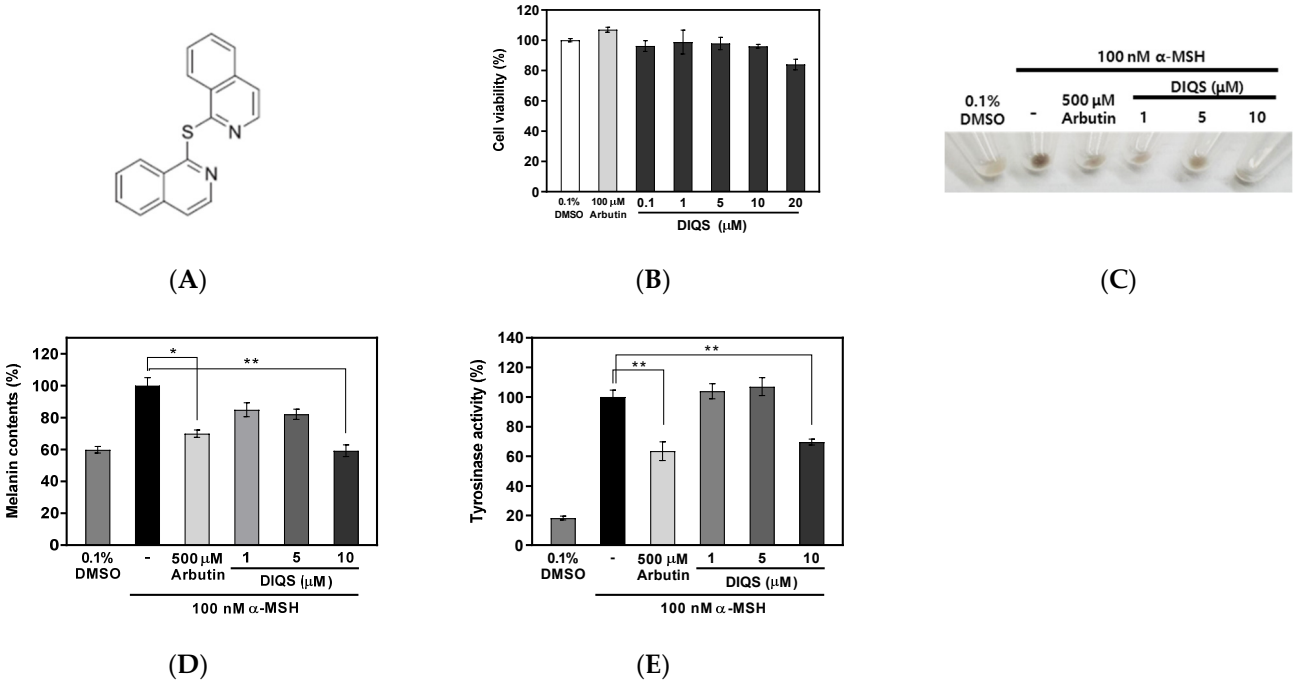

Figure 1. Di (isoquinolin-1-yl) sulfane (DIQS) induced an anti-melanogenic effect in B16F10 murine melanoma cells. (**A**) The chemical structure of DIQS is shown. (**B**) B16F10 cells were treated with various concentrations of DIQS for 48 h. The viability of B16F10 cells was determined using the Cell counting kit-8. (**C**) The cells were harvested to measure melanin content. Cell lysates were photographed prior to measurement of the melanin content. (**D**) Melanin content in B16F10 cells was significantly inhibited by DIQS treatments. (**E**) Tyrosinase activity induced by α-MSH was decreased in B16F10 cells at a concentration of 10 μM after 48 h of DIQS treatment. DIQS inhibited tyrosinase activity in α-MSH-stimulated B16F10 cells. Data are means ± standard deviation (SD). * $p < 0.05$; ** $p < 0.01$ (vs. the α-MSH treated group).

mRNA levels of *MITF*, tyrosinase, *TRP-1*, and *TRP-2* were significantly decreased by DIQS treatment at a concentration of 10 μM (Figure 2A). The effects of DIQS on *MITF*, tyrosinase, *TRP-1*, and *TRP-2* expression were determined by Western blot analysis (Figure 2B). *MITF* protein levels were decreased by 5 and 10 μM DIQS treatment. The amount of tyrosinase was clearly reduced by treatment with 10 μM DIQS. The increased protein expression of *TRP-1* and *TRP-2* induced by α-MSH was slightly decreased by DIQS treatment. These results suggest that DIQS suppressed *MITF* and tyrosinase at the mRNA and protein levels, leading to reduced tyrosinase activity and melanin content at the cellular level. To further confirm the pathways involved in the anti-melanogenic effects of DIQS, we analyzed CREB and MAPK levels by Western blotting. As shown in Figure 2C, the level of p-CREB was markedly reduced by 10 μM DIQS compared with the level in α-MSH-induced B16F10 cells. The phosphorylation of *p38* and *JNK* was reduced at the same concentration of DIQS, and the phosphorylation of *ERK* was slightly increased. These results were consistent with substances having anti-melanogenic effects [26]. Our results indicate that the anti-melanogenic activity of DIQS was associated with decreases in p-p38 and p-CREB levels, and that the anti-melanogenic effects of DIQS are related to both p-CREB inhibition and the activity of MAPKs such as *p38*, *ERK*, and *JNK*.

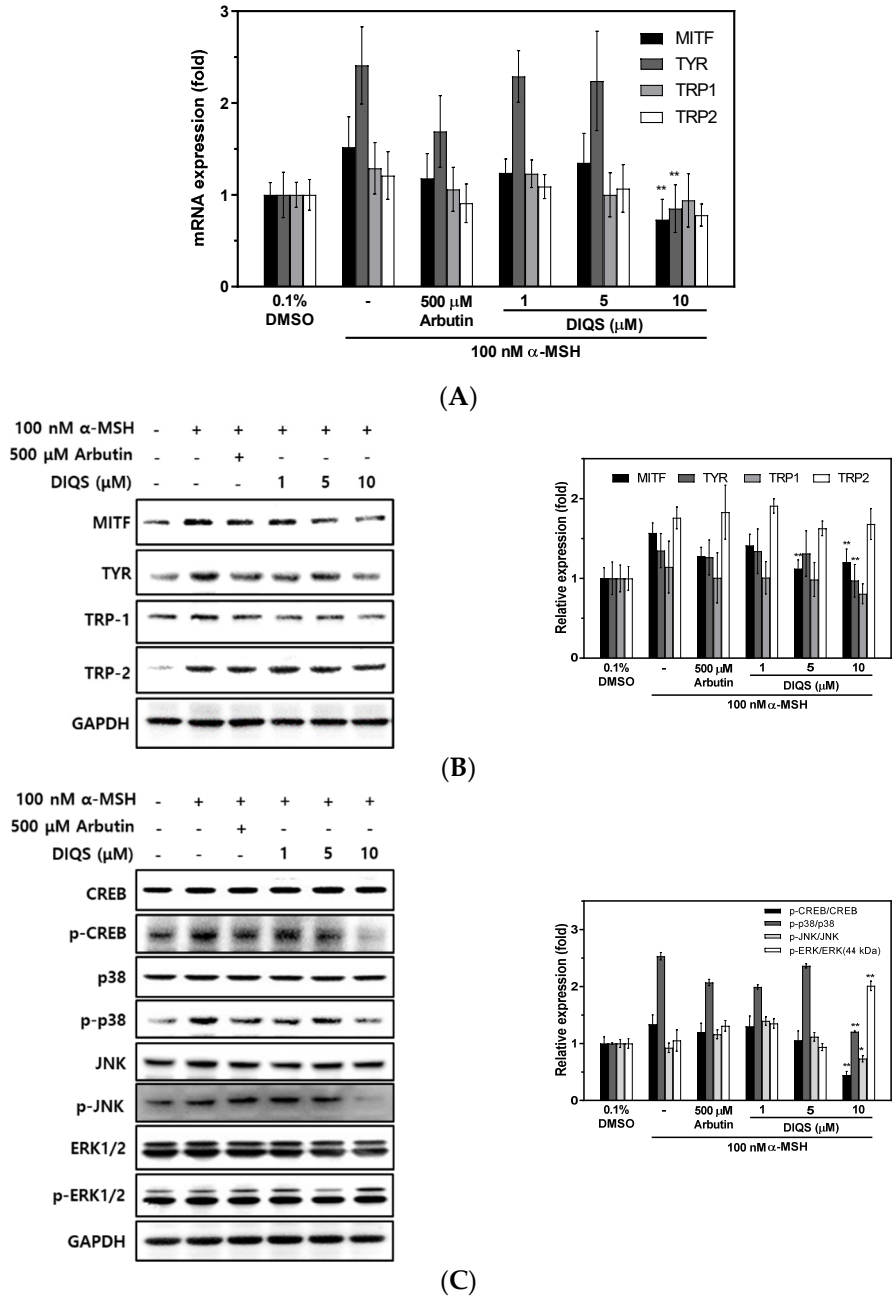

Figure 2. DIQS affected the expression of melanogenesis-related proteins and upstream signaling pathways. (**A**) B16F10 cells were incubated with the indicated concentrations of DIQS for 48 h. mRNA levels of the melanogenesis-related genes *MITF*, tyrosinase, *TRP-1*, and *TRP-2* were determined by qRT-PCR. The results are expressed relative to untreated cells after normalization against the *GAPDH* level. (**B**) B16F10 cells were incubated with the indicated concentrations of DIQS for 48 h. Arbutin was used as a positive control. The protein levels of *MITF*, tyrosinase, *TRP-1*, and *TRP-2* were determined by Western blot analysis. (**C**) Phosphorylation levels of CREB and MAPKs were also determined by Western blot analysis. The phosphorylation level of each MAPK is expressed relative to the respective total protein level. Protein levels were quantified using myImageAnalysis v2.0 software. Data are means ± SD. * $p < 0.05$ and ** $p < 0.01$ (vs. the α-MSH-treated group).

3.3. DIQS Blocked Melanin Synthesis in Pigmented Human Skin Tissue

We used the reconstituted human melanocyte model Neoderm-ME to test the safety and efficacy of skin whitening [14]. Neoderm-ME was treated with DIQS and arbutin and incubated at 37 °C in a 5% CO_2 incubator for 5 days. Microscopic evaluation revealed

that DIQS and arbutin did not decrease the number of melanocytes (Figure 3A). However, DIQS exhibited stronger inhibition of tyrosinase enzymatic activity than that observed in the DMSO and arbutin treatment groups (Figure 3B). DIQS also showed reduced melanin content in the artificial tissue (Figure 3C).

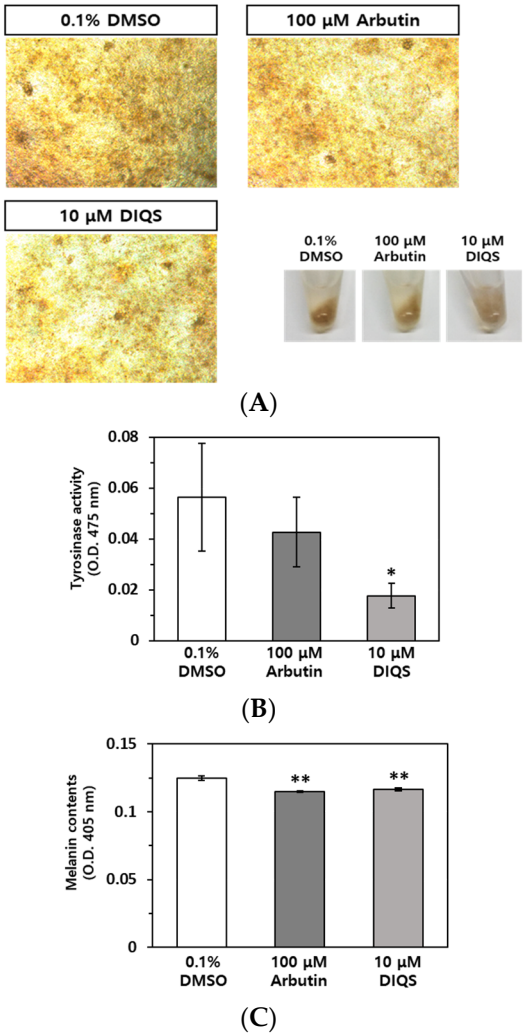

Figure 3. DIQS treatment inhibited melanin synthesis in pigmented human skin tissue. (**A**) Representative images of cultured human skin tissue. Melanin pellets were prepared as described in the Materials and Methods, and photographs were taken prior to measurement of melanin content. (**B**) Melanin content in the Neoderm-ME model was inhibited by 10 μM DIQS. (**C**) Tyrosinase activity in the Neoderm-ME model was inhibited by 10 μM DIQS. Data are means ± SD. * $p < 0.05$ and ** $p < 0.01$ (vs. the α-MSH-treated group).

3.4. DIQS Inhibited Melanogenesis in Zebrafish Embryos

Zebrafish larvae have been used as phenotype-based models to evaluate anti-melanogenic effects. To determine the effectiveness of DIQS as an anti-melanogenic compound, we compared its effects with the tyrosinase inhibitors arbutin and PTU [27,28] as positive controls. DIQS effectively reduced melanogenesis in zebrafish embryos in a dose-dependent manner compared with the DMSO group. Developing zebrafish exhibited de-pigmentation after treatment with 5 μM DIQS (Figure 4A, upper). Extracts were prepared from the zebrafish embryos by centrifugation, and the pellet colors were compared visually (Figure 4A, lower). The results confirmed that melanin content was clearly reduced at a DIQS concentration of 5 μM. Melanin content was quantified by spectrophotometry and was found to have decreased significantly as the concentration of DIQS increased (Figure 4B). Next, we exam-

ined the enzymatic activity of tyrosinase in whole embryos followed by DIQS treatment. DIQS treatment decreased tyrosinase enzymatic activity in zebrafish embryos (Figure 4C). These data suggest that DIQS acts as a melanogenesis inhibitor by inhibiting tyrosinase enzymatic activity.

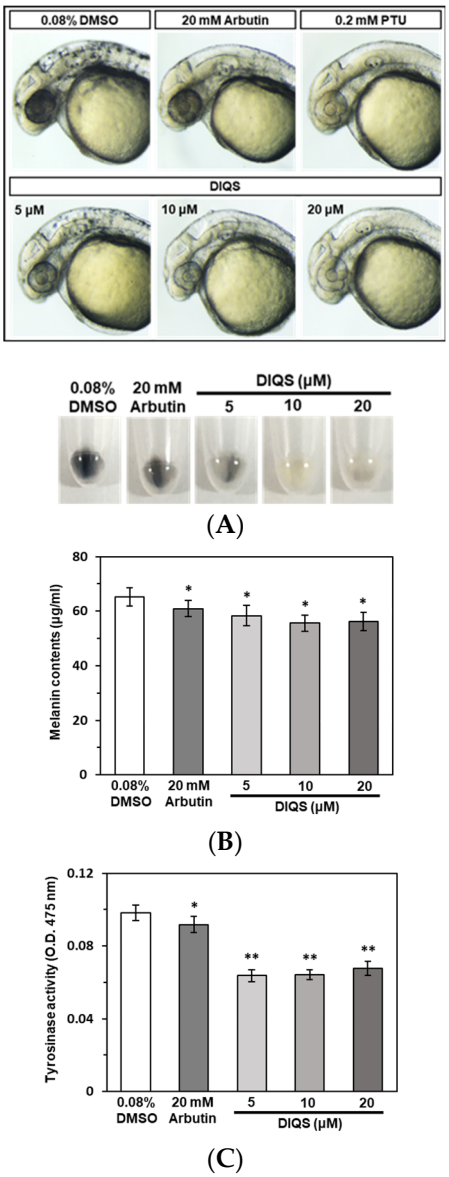

Figure 4. DIQS treatment inhibited melanogenesis in zebrafish embryos. Synchronized embryos were treated with 0.08% dimethyl sulfoxide (DMSO), 0.2 mM PTU, 20 mM arbutin, and various concentrations of DIQS. (**A**) Zebrafish embryos were photographed using the Leica MZ10 F stereomicroscope and edited using the Leica Application Suite software. Lysates from zebrafish embryos were prepared as described in the Materials and Methods. Photographs were taken prior to measurement of the melanin content. (**B**) Melanin content in zebrafish embryos was dose-dependently inhibited by DIQS treatment. (**C**) For tyrosinase activity measurements, 2500 μg total protein was incubated with 100 μL of 1 mM L-DOPA for 1 h at 37 °C, and the absorbance was measured at 495 mm. Data are means ± SD. * $p < 0.05$ and ** $p < 0.01$ (vs. the DMSO-treated group).

3.5. DIQS Blocked Melanin Synthesis in Pigmented Zebrafish Embryos

We also tested the effects of DIQS treatment on zebrafish embryos with complete melanopore formation to determine whether DIQS reduces melanin content via melanopore damage. Because zebrafish embryo melanophores are completely differentiated and con-

tinuously produced by 2 days post-fertilization [29], we exposed zebrafish embryos at 2.5 days post-fertilization to DIQS for 12 h. As a result, DIQS did not seem to change the shape of melanophores or decrease the number of melanophores (Figure 5A). However, tyrosinase activity and melanin content were decreased compared with the DMSO and arbutin treatment groups (Figure 5B,C). These results indicate that newly synthesized melanin is attenuated without toxicity in fully pigmented cells following DIQS treatment. The initial step of melanin synthesis is hydroxylation of tyrosine to DOPA, followed by the oxidation of DOPA to DOPAquinone. Tyrosinase is the key enzyme involved in this biosynthesis pathway via the binding of copper ions [8]. To determine whether DIQS affects these biosynthesis pathways, we quantitatively analyzed tyrosine and DOPA in zebrafish embryos using liquid chromatography–tandem mass spectrometry (LC–MS/MS). We determined the total amounts of tyrosine and L-DOPA in the zebrafish embryos and calculated the L-DOPA/tyrosine ratio for tyrosinase activity. DIQS treatment for 48 h decreased the L-DOPA/tyrosine ratio in a dose-dependent manner compared with DMSO. As a positive control, PTU treatment also decreased the L-DOPA/tyrosine ratio (Figure 5D). These data suggest that DIQS blocks the conversion of tyrosine to DOPA by inhibiting tyrosinase activity.

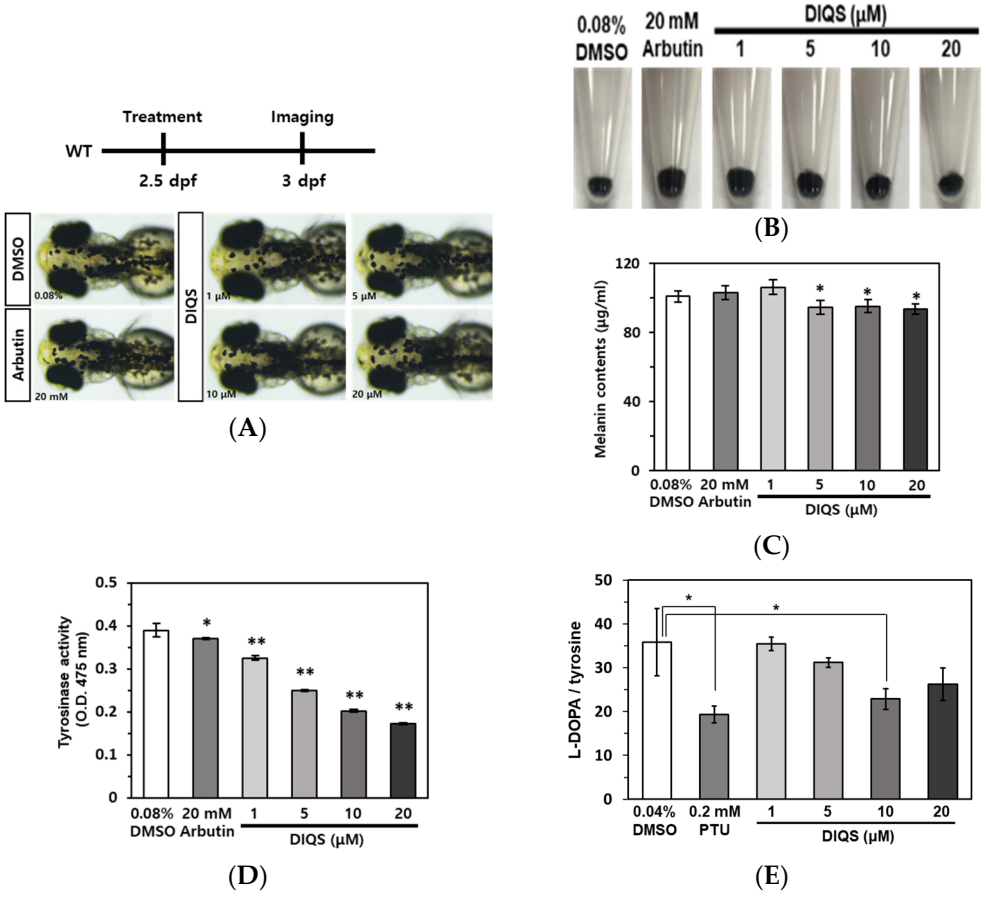

Figure 5. DIQS treatment attenuated melanin content without melanophore damage. (**A**) Zebrafish were treated with DIQS at 2.5 days post-fertilization to evaluate its effects on melanophore morphology. Melanophores in DMSO-, arbutin-, and DIQS-treated zebrafish embryos were visualized using the Leica MZ10 F stereomicroscope. (**B**) Melanin pellets were prepared and photographed for comparisons between groups. (**C**) Melanin content was analyzed in zebrafish embryos. (**D**) Tyrosinase activity was measured as described in the Materials and Methods. (**E**) Tyrosine and L-DOPA in zebrafish embryos were quantitatively analyzed by liquid chromatography–tandem mass spectrometry (LC–MS/MS). Data are L-DOPA/tyrosine ratios. * $p < 0.05$; ** $p < 0.01$ (vs. the DMSO-treated group).

3.6. DIQS Treatment Did Not Irritate Human Skin or Eye Tissues

The use of test animals is prohibited in all tests involved in the development of cosmetics in European countries [30]. Various artificial skin [31–33] and cornea models [34,35] have been developed to mimic the structure and function of human tissues. We evaluated the irritation effect of DIQS in human tissues and in reconstituted human skin and eye tissues (Neoderm-ED and -CD, respectively). In the skin irritation test, the cell viability in the reconstituted tissues was 3.52 ± 0.19% in the 5% SDS-treated group, which served as a positive control. The effect of DIQS on the cell viability in the reconstituted tissues was evaluated at concentrations of 10, 20, and 50 μM. DIQS resulted in dose-dependent inhibition of viability: 95.8 ± 22.3% at 10 μM, 91.4 ± 0.76% at 20 μM, and 79.9 ± 0.26% at 50 μM (Figure 6A). At all tested concentrations, viability exceeded 50% after 60 min of exposure and 42 h of incubation [24]. The reconstituted human cornea model Neoderm-CD was used to test acute ocular irritation induced by DIQS. The cell viability of reconstituted tissues was 21.1 ± 10.3% in the 10% acetic acid treatment group, which served as a positive control. However, no significant decrease in cell viability was observed at 10, 20, or 50 μM DIQS (Figure 6B). These results suggest that DIQS is a non-corrosive or non-irritant substance for human skin and eyes.

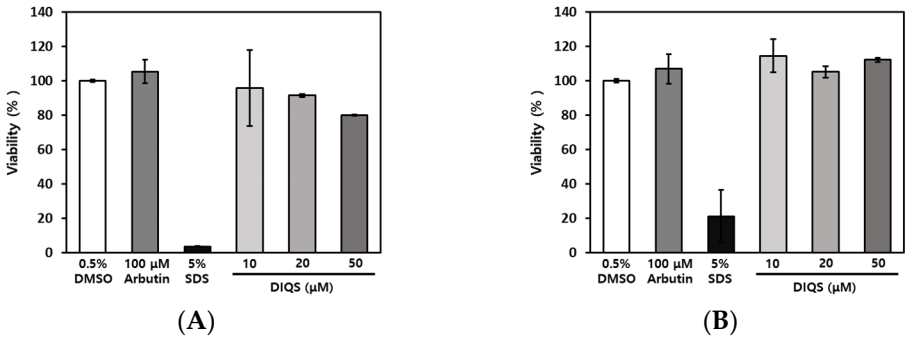

Figure 6. DIQS did not exhibit irritable effects in artificial human skin and cornea tissues. DIQS toxicity assays were performed using artificial skin and cornea models in accordance with the Organization for Economic Cooperation and Development (OECD) guidelines. (**A**) The effect of DIQS on skin irritation was tested using the Neoderm-ED reconstituted human skin model. (**B**) The effect of DIQS on acute cornea irritation was tested using the Neoderm-CD reconstituted human cornea model.

4. Discussion

Various model such as B16F10 cells, artificial skin, and zebrafish models have been used to identify the anti-melanogenic effects, toxicity, and action mechanisms of DIQS. In this study, we demonstrated the anti-melanogenic effect of DIQS using α-MSH-stimulated B16F10 cells. Tyrosinase is a key enzyme in melanin synthesis in mammalian cells [36]. The transcription of tyrosinase is regulated by *MITF* in melanogenic signaling pathways [37,38]. The expression levels of *MITF* and tyrosinase were significantly suppressed at a DIQS concentration of 10 μM in α-MSH-stimulated B16F10 cells (Figure 2). These results suggest that DIQS inhibits melanin synthesis by controlling the expression of tyrosinase by inhibiting *MITF* gene expression. To further investigate the upstream mechanisms by which DIQS inhibits melanogenesis, we examined the cAMP–PKA–CREB–*MITF*–tyrosinase axis and MAPK pathways. The MAPK family comprises three types of protein kinases: ERK, JNK, and p38. MAPKs have been reported to modulate melanogenesis [39,40], and p38 activation contributes to melanin production by activating CREB and sequentially increasing *MITF* expression [41]. The data shown in Figure 2 provide evidence that DIQS inactivates CREB, in turn inhibiting *MITF* expression. These results also suggest that DIQS shows anti-melanogenic effects by regulating the phosphorylation of ERK, JNK, and p38.

DIQS inhibits tyrosinase enzymatic activity in human tissue models and zebrafish without producing developmental defects. DIQS treatment resulted in de-pigmentation

in embryos, mainly via temporal inhibition of melanin synthesis. This de-pigmentation occurred not only in the melanophores of developing zebrafish but also in fully developed melanocytes. In our previous study, we defined the internal concentrations of chemical compounds after treatment in embryos/larvae, and the results suggested a correlation between the phenotype and chemical strength in the zebrafish model [14]. In the present study, we found that the whitening effect occurred in zebrafish at a lower concentration (5 μM) compared with that in cells. This phenomenon suggests that DIQS accumulation in zebrafish may result in melanophore exposure to high DIQS concentrations. Therefore, we also measured the actual concentration of DIQS using LC–MS/MS in zebrafish embryos after treatment. Indeed, DIQS dose-dependently accumulated in zebrafish embryos, indicating that the DIQS treatment produced an anti-melanogenic phenotype corresponding to the actual DIQS concentration in zebrafish embryos (data not shown). The amounts of tyrosine and L-DOPA after DIQS treatment were analyzed by LC–MS/MS, and a decrease in tyrosinase activity was observed. Because tyrosinase is a key enzyme catalyzing tyrosine to L-DOPA, we expected the amount of L-DOPA to be decreased by tyrosinase inhibition in the DIQS-treated embryos. After 48 h of DIQS treatment, the ratio of L-DOPA/tyrosine in zebrafish was decreased (Figure 5E). This finding indicates that DIQS mainly decreases the expression of tyrosinase and consequently retards the catalysis of tyrosine to L-DOPA.

In fact, it is very limited to measure protein levels such as various MAPK, *MITF*, tyrosinase, *TRP-1*, and *TRP-1* using the zebrafish model. Therefore, an experiment was not performed on the mechanism of action of DIQS using the zebrafish model. Instead, since zebrafish embryos are easy to observe phenotypical changes, morphological observations of melanophores containing melanin pigments were carried out. Morphological changes in melanophore were observed after exposure of DIQS to embryos in which the expression of melanin pigment was completed. In previous studies, it is known that melanophores are completely differentiated at 2 dpf during the maturation process of zebrafish embryos [29]. Therefore, melanophores were observed after exposure of DIQS to 2.5 dpf zebrafish embryos for 12 h in which melanophores were stably maintained. As a result, morphological changes in melanophores after DIQS treatment were not observed. However, we found that tyrosinase activity and melanin content were decreased compared with the DMSO and arbutin treatments (Figure 5C,D). These results suggest that DIQS may inhibit the newly synthetic process of melanin rather than reducing melanin content by slowing cell growth or inducing cell damage. In addition to zebrafish, safety tests using artificial tissue were also performed in this study. The development of skin-whitening cosmetics entails assessing the clinical efficacy of molecules and validating their safety [4]. Artificial skin tissues, human keratinocytes, or melanocytes are typically used to evaluate the safety of skin-whitening candidates [42,43]. In this study, we used reconstituted human skin and eye tissue models for irritancy testing based on OECD guidelines [24,25]. Although DIQS slightly decreased the cell viability of human skin tissue, based on OECD TG439, we concluded that DIQS was a non-irritant material.

5. Conclusions

We found that DIQS, a novel anti-melanogenic agent, inhibits melanin synthesis via the inhibition of tyrosinase enzymatic activity. We used human melanocytes, keratinocytes, and cornea tissue to demonstrate that DIQS is a non-toxic/non-irritant substance. Together, our findings suggest that DIQS is an excellent skin-whitening candidate for the cosmetic industry.

Author Contributions: Conceptualization, D.-S.S. and K.-S.H.; methodology, J.Y.Y., D.-S.S., K.-S.H. and S.S.K.; validation, D.-S.S., K.-S.H. and J.Y.Y.; formal analysis, B.H.L.; investigation, J.Y.Y., S.S.K., B.H.L. and S.H.A.; data curation, D.-S.S., K.-S.H. and J.Y.Y.; writing—original draft preparation, D.-S.S. and K.-S.H.; writing—review and editing, D.-S.S.; supervision, M.A.B. and J.H.A.; project administration, M.A.B.; funding acquisition, M.A.B. All authors have read and agreed to the published version of the manuscript.

Funding: This research was funded by grants from the Ministry of Trade, Industry and Energy, Korea (2021-10063396). This work was also partially supported by a project of Korea Research Institute of Chemical Technology (SI2131-50).

Institutional Review Board Statement: All experimental protocols involving zebrafish were approved by the Animal Care and Use Committee of the Korea Research Institute of Chemical Technology (KRICT-7B-ZF1).

Informed Consent Statement: Not applicable.

Data Availability Statement: Data are available from a publicly accessible repository.

Conflicts of Interest: The authors declare no conflict of interest.

References

1. Land, E.J.; Ramsden, C.A.; Riley, P.A. Quinone Chemistry and Melanogenesis. *DNA Sens. Inflammasomes* **2004**, *378*, 88–109. [CrossRef]
2. Wang, N.; Hebert, D.N. Tyrosinase maturation through the mammalian secretory pathway: Bringing color to life. *Pigment Cell Res.* **2006**, *19*, 3–18. [CrossRef] [PubMed]
3. Agar, N.; Young, A.R. Melanogenesis: A photoprotective response to DNA damage? *Mutat. Res. Mol. Mech. Mutagen.* **2005**, *571*, 121–132. [CrossRef] [PubMed]
4. Burger, P.; Landreau, A.; Azoulay, S.; Michel, T.; Fernandez, X. Skin Whitening Cosmetics: Feedback and Challenges in the Development of Natural Skin Lighteners. *Cosmetics* **2016**, *3*, 36. [CrossRef]
5. Silvestri, M.; Bennardo, L.; Zappia, E.; Tamburi, F.; Cameli, N.; Cannarozzo, G.; Nisticò, S.P. Q-Switched 1064/532 nm laser with picosecond pulse to treat benign hyperpigmentations: A single-center retrospective study. *Appl. Sci.* **2021**, *11*, 7478.
6. Nisticò, S.P.; Tolone, M.; Zingoni, T.; Tamburi, F.; Scali, E.; Bennardo, L.; Cannarozzo, G. A New 675 nm Laser Device in the Treatment of Melasma: Results of a Prospective Observational Study. *Photobiomodulation Photomed. Laser Surg.* **2020**, *38*, 560–564. [CrossRef]
7. Smit, N.; Vicanova, J.; Pavel, S. The Hunt for Natural Skin Whitening Agents. *Int. J. Mol. Sci.* **2009**, *10*, 5326–5349. [CrossRef]
8. Hearing, V.J. Determination of Melanin Synthetic Pathways. *J. Investig. Dermatol.* **2011**, *131*, E8–E11. [CrossRef]
9. Opdecamp, K.; Nakayama, A.; Nguyen, M.T.; Hodgkinson, C.A.; Pavan, W.J.; Arnheiter, H. Melanocyte development in vivo and in neural crest cell cultures: Crucial dependence on the Mitf basic-helix-loop-helix-zipper transcription factor. *Development* **1997**, *124*, 2377–2386.
10. Tachibana, M. MITF: A Stream Flowing for Pigment Cells. *Pigment Cell Res.* **2000**, *13*, 230–240. [CrossRef]
11. Bertolotto, C.; Buscà, R.; Abbe, P.; Bille, K.; Aberdam, E.; Ortonne, J.-P.; Ballotti, R. Different cis -Acting Elements Are Involved in the Regulation of TRP1 and TRP2 Promoter Activities by Cyclic AMP: Pivotal Role of M Boxes (GTCATGTGCT) and of Microphthalmia. *Mol. Cell. Biol.* **1998**, *18*, 694–702. [CrossRef] [PubMed]
12. Pillaiyar, T.; Manickam, M.; Jung, S.-H. Downregulation of melanogenesis: Drug discovery and therapeutic options. *Drug Discov. Today* **2017**, *22*, 282–298. [CrossRef]
13. Wu, L.-C.; Lin, Y.-Y.; Yang, S.-Y.; Weng, Y.-T.; Tsai, Y.-T. Antimelanogenic effect of c-phycocyanin through modulation of tyrosinase expression by upregulation of ERK and downregulation of p38 MAPK signaling pathways. *J. Biomed. Sci.* **2011**, *18*, 74. [CrossRef]
14. Hwang, K.-S.; Yang, J.Y.; Lee, J.; Lee, Y.-R.; Kim, S.S.; Kim, G.R.; Chae, J.S.; Ahn, J.H.; Shin, D.-S.; Choi, T.-Y.; et al. A novel anti-melanogenic agent, KDZ-001, inhibits tyrosinase enzymatic activity. *J. Dermatol. Sci.* **2018**, *89*, 165–171. [CrossRef]
15. Wangchuk, P.; Sastraruji, T.; Taweechotipatr, M.; Keller, P.; Pyne, S. Anti-inflammatory, Anti-bacterial and Anti-acetylcholinesterase Activities of two Isoquinoline Alkaloids–Scoulerine and Cheilanthifoline. *Nat. Prod. Commun.* **2016**, *11*, 1801–1804. [CrossRef]
16. Song, Y.C.; Lee, Y.; Kim, H.M.; Hyun, M.Y.; Lim, Y.Y.; Song, K.Y.; Kim, B.J. Berberine regulates melanin synthesis by activating PI3K/AKT, ERK and GSK3β in B16F10 melanoma cells. *Int. J. Mol. Med.* **2015**, *35*, 1011–1016. [CrossRef] [PubMed]
17. Mort, R.L.; Jackson, I.J.; Patton, E.E. The melanocyte lineage in development and disease. *Development* **2015**, *142*, 620–632. [CrossRef]
18. Colanesi, S.; Taylor, K.L.; Temperley, N.D.; Lundegaard, P.R.; Liu, D.; North, T.E.; Ishizaki, H.; Kelsh, R.N.; Patton, E.E. Small molecule screening identifies targetable zebrafish pigmentation pathways. *Pigment. Cell Melanoma Res.* **2012**, *25*, 131–143. [CrossRef] [PubMed]
19. Hayazaki, M.; Hatano, O.; Shimabayashi, S.; Akiyama, T.; Takemori, H.; Hamamoto, A. Zebrafish as a new model for rhododendrol-induced leukoderma. *Pigment Cell Melanoma Res.* **2021**. Epub ahead of print. [CrossRef]
20. Westerfield, M. *The Zebrafish Book: A Guide for the Laboratory Use of Zebrafish (Brachydanio rerio)*; University of Oregon Press: Eugene, OR, USA, 1995.
21. Park, P.J.; Lee, T.R.; Cho, E.G. Substance P Stimulates Endothelin 1 Secretion via Endothelin-Converting Enzyme 1 and Promotes Melanogenesis in Human Melanocytes. *J. Investig. Dermatol.* **2015**, *135*, 551–569.
22. Kim, J.H.; Baek, S.H.; Kim, D.H.; Choi, T.Y.; Yoon, T.J.; Hwang, J.S.; Kim, M.R.; Kwon, H.J.; Lee, C.H. Downregulation of Melanin Synthesis by Haginin A and Its Application to In Vivo Lightening Model. *J. Investig. Dermatol.* **2008**, *128*, 1227–1235. [CrossRef]

23. Kim, S.S.; Lee, H.-Y.; Song, J.S.; Bae, M.-A.; Ahn, S. UPLC-MS/MS-based profiling of 31 neurochemicals in the mouse brain after treatment with the antidepressant nefazodone. *Microchem. J.* **2021**, *169*, 106580. [CrossRef]
24. OECD. *Test No. 439: In Vitro Skin Irritation*; OECD: Paris, France, 2010.
25. OECD. *Test No. 492: Reconstructed Human Cornea-Like Epithelium (RhCE) Test Method for Identifying Chemicals Not Requiring Classification and Labelling for Eye Irritation or Serious Eye Damage*; OECD: Paris, France, 2019.
26. Peng, H.-Y.; Lin, C.-C.; Wang, H.-Y.; Shih, Y.; Chou, S.-T. The Melanogenesis Alteration Effects of *Achillea millefolium* L. Essential Oil and Linalyl Acetate: Involvement of Oxidative Stress and the JNK and ERK Signaling Pathways in Melanoma Cells. *PLoS ONE* **2014**, *9*, e95186. [CrossRef]
27. Choi, T.-Y.; Kim, J.-H.; Ko, D.H.; Kim, C.-H.; Hwang, J.-S.; Ahn, S.; Kim, S.Y.; Kim, C.D.; Lee, J.-H.; Yoon, T.-J. Zebrafish as a new model for phenotype-based screening of melanogenic regulatory compounds. *Pigment. Cell Res.* **2007**, *20*, 120–127. [CrossRef]
28. Peterson, R.T.; Link, B.A.; Dowling, J.E.; Schreiber, S.L. Small molecule developmental screens reveal the logic and timing of vertebrate development. *Proc. Natl. Acad. Sci. USA* **2000**, *97*, 12965–12969. [CrossRef] [PubMed]
29. Hultman, K.A.; Budi, E.H.; Teasley, D.C.; Gottlieb, A.Y.; Parichy, D.M.; Johnson, S.L. Defects in ErbB-dependent establishment of adult melanocyte stem cells reveal independent origins for embryonic and regeneration melanocytes. *PLoS Genet.* **2009**, *5*, e1000544. [CrossRef] [PubMed]
30. Faller, C.; Bracher, M.; Dami, N.; Roguet, R. Predictive ability of reconstructed human epidermis equivalents for the assessment of skin irritation of cosmetics. *Toxicol. Vitr.* **2002**, *16*, 557–572. [CrossRef]
31. Mao, J.; Zhao, L.; De Yao, K.; Shang, Q.; Yang, G.; Cao, Y. Study of novel chitosan-gelatin artificial skin in vitro. *J. Biomed. Mater. Res. A* **2003**, *64*, 301–308. [CrossRef]
32. Whang, K.-K.; Kim, M.-J.; Song, W.-K.; Cho, S. Comparative Treatment of Giant Congenital Melanocytic Nevi with Curettage or Er:YAG Laser Ablation Alone versus with Cultured Epithelial Autografts. *Dermatol. Surg.* **2005**, *31*, 1660–1667. [CrossRef]
33. You, H.-J.; Han, S.-K.; Lee, J.-W.; Chang, H. Treatment of diabetic foot ulcers using cultured allogeneic keratinocytes-A pilot study. *Wound Repair Regen.* **2012**, *20*, 491–499. [CrossRef]
34. McLaughlin, C.R.; Tsai, R.J.; Latorre, M.A.; Griffith, M. Bioengineered corneas for transplantation and in vitro toxicology. *Front Biosci.* **2009**, *14*, 3326–3337. [CrossRef] [PubMed]
35. Pfannenbecker, U.; Bessou-Touya, S.; Faller, C.; Harbell, J.; Jacob, T.; Raabe, H.; Tailhardat, M.; Alépée, N.; De Smedt, A.; De Wever, B.; et al. Cosmetics Europe multi-laboratory pre-validation of the EpiOcular™ reconstituted human tissue test method for the prediction of eye irritation. *Toxicol. Vitr.* **2013**, *27*, 619–626. [CrossRef] [PubMed]
36. Tief, K.; Hahne, M.; Schmidt, A.; Beermann, F. Tyrosinase, the Key Enzyme in Melanin Synthesis, is Expressed in Murine Brain. *JBIC J. Biol. Inorg. Chem.* **1996**, *241*, 12–16. [CrossRef]
37. Du, J.; Miller, A.J.; Widlund, H.R.; Horstmann, M.A.; Ramaswamy, S.; Fisher, D.E. MLANA/MART1 and SILV/PMEL17/GP100 Are Transcriptionally Regulated by MITF in Melanocytes and Melanoma. *Am. J. Pathol.* **2003**, *163*, 333–343. [CrossRef]
38. Goding, C.R. Mitf from neural crest to melanoma: Signal transduction and transcription in the melanocyte lineage. *Genes Dev.* **2000**, *14*, 1712–1728.
39. Hirata, N.; Naruto, S.; Ohguchi, K.; Akao, Y.; Nozawa, Y.; Iinuma, M.; Matsuda, H. Mechanism of the melanogenesis stimulation activity of (−)-cubebin in murine B16 melanoma cells. *Bioorg. Med. Chem.* **2007**, *15*, 4897–4902. [CrossRef]
40. Kim, D.-S.; Jeong, Y.-M.; Park, I.-K.; Hahn, H.-G.; Lee, H.-K.; Kwon, S.-B.; Jeong, J.H.; Yang, S.J.; Sohn, U.D.; Park, K.-C. A New 2-Imino-1,3-thiazoline Derivative, KHG22394, Inhibits Melanin Synthesis in Mouse B16 Melanoma Cells. *Biol. Pharm. Bull.* **2007**, *30*, 180–183. [CrossRef]
41. Singh, S.K.; Sarkar, C.; Mallick, S.; Saha, B.; Bera, R.; Bhadra, R. Human placental lipid induces melanogenesis through p38 MAPK in B16F10 mouse melanoma. *Pigment Cell Res.* **2005**, *18*, 113–121. [CrossRef]
42. Inoue, Y.; Hasegawa, S.; Yamada, T.; Date, Y.; Mizutani, H.; Nakata, S.; Matsunaga, K.; Akamatsu, H. Analysis of the Effects of Hydroquinone and Arbutin on the Differentiation of Melanocytes. *Biol. Pharm. Bull.* **2013**, *36*, 1722–1730. [CrossRef]
43. Osborne, R.; Perkins, M. In vitro skin irritation testing with human skin cell cultures. *Toxicol. Vitr.* **1991**, *5*, 563–567. [CrossRef]